

1 Results from a Prototype Chicane-Based  
2 Energy Spectrometer for a Linear Collider

3 A. Lyapin<sup>a,\*</sup>, H.J. Schreiber<sup>b</sup>, M. Viti<sup>b</sup>, C. Adolphsen<sup>c</sup>, R. Arnold<sup>c</sup>,  
4 S. Boogert<sup>d</sup>, G. Boorman<sup>d</sup>, F. Gournaris<sup>a</sup>, V. Duginov<sup>e</sup>, C. Hast<sup>c</sup>,  
5 M. Hildreth<sup>g</sup>, C. Hlaing<sup>h</sup>, F. Jackson<sup>i</sup>, O. Khainovsky<sup>h</sup>, Y. Kolomensky<sup>h</sup>,  
6 S. Kostromin<sup>e</sup>, B. Maiheu<sup>a</sup>, D. McCormick<sup>c</sup>, D. J. Miller<sup>a</sup>, N. Morozov<sup>e</sup>,  
7 T. Orimoto<sup>h,j</sup>, M. Slater<sup>f</sup>, Z. Szalata<sup>c</sup>, M. Thomson<sup>f</sup>, D. Ward<sup>f</sup>, M. Wing<sup>a</sup>,  
8 M. Woods<sup>c</sup>

9 <sup>a</sup>University College London, London, UK

10 <sup>b</sup>Deutsches Elektronen Synchrotron DESY Hamburg and Zeuthen, Germany

11 <sup>c</sup>SLAC National Accelerator Laboratory, Menlo Park, California, USA

12 <sup>d</sup>Royal Holloway, University of London, Egham, UK

13 <sup>e</sup>Joint Institute for Nuclear Research, Dubna, Moscow Region, Russia

14 <sup>f</sup>University of Cambridge, Cambridge, UK

15 <sup>g</sup>University of Notre Dame, Notre Dame, Indiana, USA

16 <sup>h</sup>University of California and Lawrence Berkeley National Laboratory, Berkeley,  
17 California, USA

18 <sup>i</sup>Daresbury Laboratory, Daresbury, UK

19 <sup>j</sup>California Institute of Technology, Pasadena, California, USA

---

20 **Abstract**

21 The International Linear Collider and other proposed high energy  $e^+e^-$   
22 machines aim to measure with unprecedented precision Standard Model  
23 quantities and new, not yet discovered phenomena. One of the main re-  
24 quirements for achieving this goal is a measurement of the incident beam  
25 energy with an uncertainty of  $10^{-4}$  or less. This article presents the analysis  
26 of data from a prototype energy spectrometer commissioned in 2006–2007  
27 in SLAC’s End Station A beamline. The prototype was a 4-magnet chi-  
28 cane equipped with beam position monitors measuring small changes of the  
29 beam orbit through the chicane at different beam energies. An energy reso-  
30 lution close to  $5 \cdot 10^{-4}$  was estimated, which, however, needs to be improved  
31 for a linear collider. We also report on the operational experience with the  
32 chicane-based spectrometer and suggest ways of improving its performance.

33 *Keywords:* Energy measurement, Energy Spectrometer, Cavity Beam

---

\*Corresponding Author. HEP Group, University College London, Gower Street, WC1E  
6BT, London, United Kingdom. Tel: +44 (0)20 7679 3454; Fax: +44 (0)20 7679 7145.

Email address: [al@hep.ucl.ac.uk](mailto:al@hep.ucl.ac.uk) (A. Lyapin)

<sup>1</sup>This work was supported by the Commission of the European Communities under the  
6th Framework Programme “Structuring the European Research Arm,” contract number  
RIDS-011899 and by the Science and Technology Facilities Council (STFC)

<sup>2</sup>This work was supported by the U.S. Department of Energy under contract DE-AC02-  
76SF00515

<sup>3</sup>This work was supported by the U.S. Department of Energy under contract DE-FG02-  
03ER41279

## 36 1. Introduction

37 The physics potential of the next  $e^+e^-$  Linear Collider depends greatly  
38 on precision energy measurements of the electron and positron beams at the  
39 interaction point (IP). Beam energy measurements are mandatory for the  
40 precision determination of the fundamental properties of particles created  
41 in the processes of interest. For example, measuring the top mass to order  
42 of 100 – 200 MeV or measuring the Standard Model Higgs mass to about  
43 50 MeV using the Higgs-strahlung process requires the luminosity-weighted  
44 collision energy to be known to a level of  $(1 - 2) \cdot 10^{-4}$  to avoid this being  
45 the dominant uncertainty [1]. Incoming beam energy ( $E_b$ ) measurements are  
46 a critical component to  $\sqrt{s}$  determination as it sets the overall energy scale  
47 for the collision process.

48 The strategy proposed in the International Linear Collider (ILC) design  
49 report [2] is to have redundant beam-based measurements capable of achiev-  
50 ing a  $10^{-4}$  relative precision on a single beam, which would be available in  
51 real time as a diagnostic tool to the operators. Also, physics reference chan-  
52 nels such as  $e^+e^- \rightarrow \mu^+\mu^-\gamma$  where the muons are resonant with the known  
53 Z-mass are expected to provide valuable cross-checks of the collision energy  
54 scale, but only long after the data have been recorded.

55 The primary method planned to perform  $E_b$  measurements at the ILC is  
56 a non-invasive energy spectrometer using beam position monitors (BPMs).  
57 The proposed setup is similar to that used for calibrating the energy scale for  
58 the W-mass measurement at LEP-II [3]. At the ILC, however, the parame-  
59 ters of the spectrometer are tightly constrained to provide limited emittance  
60 dilution at the highest ILC energy  $E_b = 500$  GeV.

61 Initially, a 3-magnet chicane located upstream of the interaction point  
62 just after the energy collimators of the beam delivery system (BDS) was  
63 proposed [4]. However, the baseline ILC spectrometer design uses two dipole  
64 magnets to produce a beam displacement  $x$ , while two more magnets return  
65 the beam to the nominal beam orbit. For such a chicane, the beam energy  
66 is then given by

$$E_b = \frac{c \cdot e \cdot L}{x} \int_{\text{magnet}} B \, dl, \quad (1)$$

67 where  $L$  is the distance between the first two magnets,  $\int B \, dl$  the integral  
 68 of the magnetic field in each magnet,  $c$  the speed of light and  $e$  the electric  
 69 charge of the electron.

70 The 4-magnet chicane avoids spurious beam displacement signals in the  
 71 BPMs due to beam tilts, and thus systematic errors in  $E_b$  measurements. For  
 72 this reason, a 4-magnet spectrometer, which maintains the beam axially with  
 73 respect to the axis of the cavity BPMs, seems preferable to a more conven-  
 74 tional 3-magnet chicane. In both cases the magnetic field in the spectrometer  
 75 chicane can be recorded and reversed for studying systematic effects without  
 76 changing the beam direction downstream of the spectrometer.

77 A dispersion of 5 mm at the centre of the chicane can be introduced  
 78 routinely without a significant degradation of the beam emittance due to  
 79 synchrotron radiation. When operating a fixed dispersion of 5 mm over the  
 80 whole energy range, a BPM resolution better than  $0.5 \, \mu\text{m}$  is needed. This  
 81 resolution can be achieved with cavity BPMs [5]. Since the spectrometer  
 82 bending magnets need to operate at low fields when running the ILC at  
 83 the Z-pole, the magnetic field measurement may not be accurate enough  
 84 to provide the required level of precision. A significantly improved BPM  
 85 resolution would, however, allow the magnets to be run at the same field for  
 86 both the Z-pole and highest energy operation.

87 An absolute energy measurement requires that the beam orbit measure-  
 88 ment is referenced to the orbit with no field applied. Unfortunately, the  
 89 residual fields still have an impact on the beam orbit at a level that may af-  
 90 fect the overall beam energy accuracy. There is an ongoing R&D program to  
 91 determine how to perform accurate field measurements for very low magnetic  
 92 fields [6].

93 Some original energy resolution studies of the SLAC prototype 4-magnet  
 94 chicane were presented in ref. [7]. The analysis used calibrated beam position  
 95 readings but revealed that due to small differences between the magnets in  
 96 the chicane the beam inclination also needs to be considered. The analysis  
 97 has here been extended by using complex BPM readings that contain the in-  
 98 formation on both the beam offset and inclination. This approach eliminates  
 99 the need for position calibration of the BPMs, while the whole system can  
 100 be calibrated by means of an energy scan.

101 In this publication we estimate the resolution of the spectrometer to com-  
102 pare it with the result of  $8.5 \cdot 10^{-4}$  measured in [7]. We also consider the im-  
103 pact of different systematics on the energy measurement in order to improve  
104 the resolution to below the  $10^{-4}$  level in future experiments.

## 105 **2. Test Beam Setup and Spectrometer Hardware Configuration**

106 A prototype test setup for a 4-magnet chicane was commissioned in 2006  
107 (the T-474 experiment) and extended in 2007 (the T-491 experiment) in the  
108 End Station A (ESA) beamline at the SLAC National Accelerator Labora-  
109 tory [8].

110 In our experiments the electron beam generated by the main Linear Ac-  
111 celerator at SLAC was transported to the ESA experimental area through the  
112 300 m long transfer line A including bending and focusing magnets, and di-  
113 agnostic instruments such as stripline and RF cavity BPMs, charge sensitive  
114 toroids, a synchrotron light monitor, profile screens and diodes. The SLAC  
115 linac provided single bunches at 10 Hz and a nominal energy of 28.5 GeV, a  
116 bunch charge of  $1.6 \cdot 10^{10}$  electrons, a bunch length of 500  $\mu\text{m}$  and an energy  
117 spread of 0.15%, i.e. a beam with properties similar to the ILC expectations  
118 at the highest energy currently available for electrons.

119 These beam parameters allowed us to test the capabilities of the proposed  
120 spectrometer under realistic conditions. Two feedback systems were in place  
121 for the ESA beam: one for its position and one for the energy. The position  
122 feedback stabilised the beam position and angle using cavity BPMs and cor-  
123 rector magnets upstream of the ESA area. The energy feedback stabilised  
124 the energy by controlling the phase of the klystrons, and thus the accelerat-  
125 ing gradient, in one of the linac sections. The energy feedback was also used  
126 for offsetting the energy from the nominal value in approximately 50 MeV  
127 steps within a  $\pm 100$  MeV range, thus providing a rough energy calibration  
128 for the spectrometer.

129 Remaining beam energy drifts change the beam orbit through the transfer  
130 line, resulting in increased beam losses as the trajectory wanders off the op-  
131 timal one. Monitoring these losses and correcting for the drifts manually, the  
132 linac operators kept the beam energy within a  $\pm 1\%$  range around 28.5 GeV  
133 during the run.

134 The setup, as schematically shown in fig. 1, includes four bending magnets  
135 denoted as 3B1, 3B2, 3B3 and 3B4, forming a chicane in the horizontal plane  
136 and high-precision cavity BPMs upstream, downstream and in between the

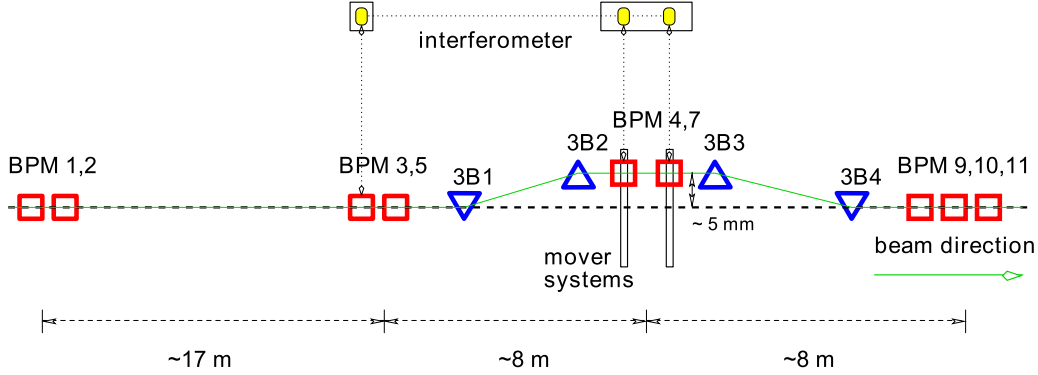


Figure 1: Schematic representation of the prototype spectrometer in ESA.

137 dipole magnets. Two of them (BPMs 4 and 7) in the middle of the chicane  
 138 were instrumented with precision movers. When the magnets were turned  
 139 on, these BPMs were mechanically moved to ensure the beam offset fits the  
 140 dynamic range of the BPM electronics. These movers were also used for  
 141 position calibrations. Horizontal positions of three monitors (BPMs 5, 4 and  
 142 7) were monitored with a Zygo interferometer [9].

143 The 10D37 magnets from the old SPEAR injection beamline, refurbished  
 144 for the use in the chicane, are 37" long, 10" wide on the pole faces and have  
 145 a 3" gap. They were run in series from a single power supply to minimise  
 146 relative drifts. The magnets were studied during a set of measurements in  
 147 the SLAC Magnet Measurement Laboratory. Magnetic field maps of the  
 148 vertical field component  $B_y$  were taken using NMR and Hall probes, while  
 149 each  $\int B dl$  was measured using a flip coil, which was calibrated against a  
 150 moving wire system. Stability and reproducibility were at the focus of these  
 151 measurements. Details of the field measurements can be found in [7, 10, 11].

152 In situ at ESA, two NMR probes with different, but overlapping working  
 153 ranges and initially also one Hall probe were installed in the first magnet  
 154 3B1, while one NMR probe was positioned in each of the other three mag-  
 155 nets, so that field integral values could be monitored. In the test data runs,  
 156 the nominal magnetic field was 0.117 T·m which corresponds to a magnet  
 157 operation at 150 A. The stray field outside the magnets in the middle of the  
 158 chicane was monitored using two low-field fluxgate magnetometers. One was  
 159 placed on the girder to obtain the horizontal ( $x$ ) and vertical ( $y$ ) field com-  
 160 ponents and the other on the beam pipe measuring the  $y$ -component only.

161 Properties of the probes and the fluxgate monitors are summarised in fig. 2.

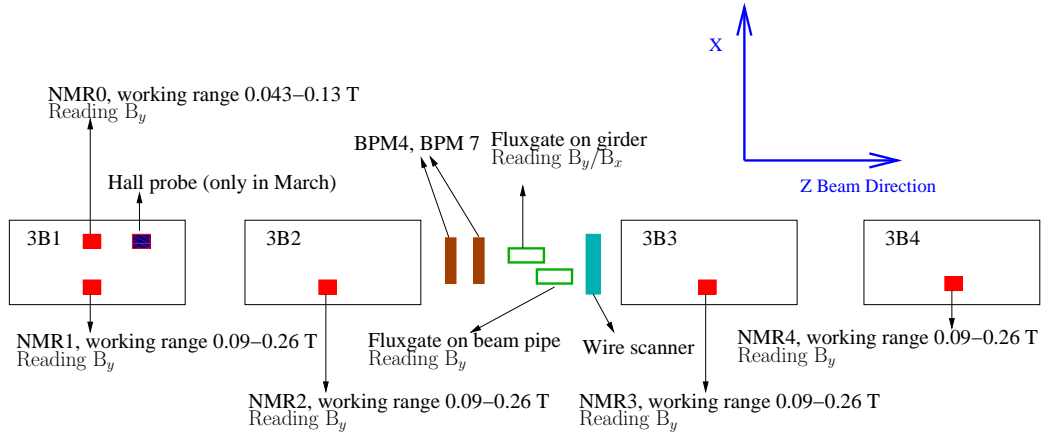


Figure 2: Magnetic field diagnostics in the spectrometer chicane.

162 The NMR probes were multiplexed sharing the same readout unit. Sev-  
 163 eral readings were obtained for each probe before switching to the next one,  
 164 each internally averaged over 2.5 s. Due to multiplexing, the NMR data  
 165 for each probe was available for about 20 s with longer than a minute gap  
 166 between the series of readings, so that only very slow variations could be  
 167 tracked reliably.

168 In order to measure the beam orbit, 8 cavity BPMs, all operating in  
 169 the S-band of the RF, were installed. Three of them were SLAC prototype  
 170 ILC BPMs (3, 4, 5) using cylindrical cavities with  $x$ - and  $y$ -waveguides for  
 171 the dipole mode coupling and monopole mode suppression. Each of the five  
 172 SLAC linac-type BPMs (1, 2, 9, 10, and 11) consists of three cavities: two  
 173 rectangular cavities for  $x$  and  $y$  separately to avoid  $x$ - $y$  couplings, and one  
 174 cylindrical cavity to provide charge and phase information. BPM 7 was a  
 175 dedicated ILC prototype designed and manufactured in the UK for the use  
 176 in the spectrometer. Unfortunately, this monitor could not be used in the  
 177 analysis due to manufacturing problems [12]. Details on the performance of  
 178 the BPM system and the A-line configuration can be found in [5].

179 BPMs 12 and 24 are placed in the bending arc region of the A-line, where  
 180 horizontal dispersion reaches several meters. For our experiment they were  
 181 instrumented with the same high-sensitivity electronics as all other BPMs in  
 182 the ESA beamline, so that the energy measurements in the A-line and in the

183 chicane could be performed simultaneously and cross-checked against each  
184 other.

### 185 **3. Performance of the Prototype Spectrometer**

#### 186 *3.1. Reconstruction of the beam orbit in the middle of the chicane*

187 As the chicane magnets bend the beam in the  $x$ -direction, we are mainly  
188 interested in the horizontal beam position and angle, and, unless specified  
189 otherwise, we refer to the  $x$ -coordinate throughout this section.

190 The offset of the beam trajectory in the middle of the chicane has to  
191 be measured with respect to the nominal orbit position reconstructed using  
192 BPMs outside of the chicane. In order to predict the readings of BPM 4 we  
193 took data with zero current in the magnets and selected a “quiet period”,  
194 when neither the beam nor the hardware settings were altered. Data from  
195 a run with magnets on could also be used for relative measurements and  
196 would result in a better prediction, however, due to the residual dispersion  
197 in the beamline, beam positions before and in the middle of the chicane are  
198 correlated. Hence, only data from a run with magnets off were used.

199 BPMs 9, 10 and 11 were not used for the prediction because, when mag-  
200 nets are on, the impact of the chicane on the beam orbit is not fully com-  
201 pensated, and the beam offset in these BPMs is energy-correlated.

202 Due to alignment errors, there is also a correlation between the vertical  
203 beam position and angle before the chicane and the horizontal beam position  
204 and angle in the mid-chicane. Therefore, both  $x$ - and  $y$ -readings from the  
205 BPMs upstream of the chicane ( $x_1, x_2, x_3, x_5, y_1, y_2, y_3$  and  $y_5$ ) were used  
206 in the analysis.

207 In our system, signals generated by the BPMs were digitised and stored  
208 in data files for each event, i.e. for each beam trigger. They are digitally  
209 converted to the baseband in the analysis [5]. A complex digital local os-  
210 cillator signal allows decoding of both the amplitude and the phase of the  
211 signal’s phasor along the waveform. Sampled at a point close to the peak and  
212 normalised by the phasor from the reference cavity, the converted waveforms  
213 give the real, in-phase (I), value and the imaginary, quadrature (Q), value,  
214 which contain the information on the beam offset as well as the inclination.

215 In order to reconstruct the beam orbit in the mid-chicane, the I and Q  
216 values from BPM 4 are correlated to the I and Q values from the upstream  
217 BPMs. We applied the Singular Value Decomposition (SVD) method [13] to  
218 several thousands of readings. Inversion of the matrix of the measured I and

219 Q values for the selected BPMs provides a vector of coefficients, which relate  
 220 the Is and Qs of each BPM,  $i$ , to those of BPM 4 so that a prediction can  
 221 be made:

$$I_{\text{BPM4}} = \alpha_0 + \sum_i \alpha_i^{(I)} \cdot I_i + \sum_i \alpha_i^{(Q)} \cdot Q_i, \quad (2)$$

$$Q_{\text{BPM4}} = \beta_0 + \sum_i \beta_i^{(I)} \cdot I_i + \sum_i \beta_i^{(Q)} \cdot Q_i, \quad (3)$$

222 where  $\alpha_{0,i}$  and  $\beta_{0,i}$  are the SVD coefficients.

223 The difference between the predicted and the measured values is the resid-  
 224 ual. In our case, the RMS residual is the precision of the orbit prediction  
 225 and the resolution of BPM 4 added in quadrature. It sets the limit on the  
 226 spectrometer resolution. The measured and predicted values for I and Q are  
 227 plotted against each other in fig. 3. The points in these plots lie around  
 228 the  $y = x$  solid lines, which means the prediction works correctly. The his-  
 229 tograms in the bottom part of fig. 3 show the residuals, for both the I and  
 230 Q values.

231 It is clear that the I and Q residuals for BPM 4 are small compared  
 232 to the average I and Q values, but the results in fig. 3 are still hard to  
 233 interpret quantitatively. In order to set a scale we used the mover scan data.  
 234 During the mover scan BPM 4 was moved in 0.25 mm steps from  $-0.5$  to  
 235  $+0.5$  mm off the nominal position. The precision of the mover system is  
 236 about 10  $\mu\text{m}$ , but the moves can also be observed by the interferometer with  
 237 a sub-micrometre precision. Fig. 4 shows the scan data as well as the position  
 238 residual, which was calculated for the data used in the SVD computations  
 239 above. A position residual of 2.73  $\mu\text{m}$  was determined, which is close to the  
 240 estimate in [7] (2.3  $\mu\text{m}$ ). The difference can be explained by softer applied  
 241 cuts and a different minimisation algorithm.

242 The residual is larger than our earlier published value [5], which was close  
 243 to 1  $\mu\text{m}$ . This is due to the movement of BPM 4 from its original location  
 244 between BPMs 3 and 5 to the middle of the chicane and exclusion of BPMs  
 245 9, 10 and 11 from this analysis. Therefore, BPM 4, which was previously in  
 246 the “centre of gravity”, here is at the edge of the BPM system. Clearly, the  
 247 precision of the orbit reconstruction at BPM 4 was affected.

248 Together with the 5 mm nominal beam offset in the middle of the chicane  
 249 for magnets on, the 2.73  $\mu\text{m}$  precision of the BPM system sets an energy  
 250 resolution limit of  $5.5 \cdot 10^{-4}$  for our spectrometer prototype.



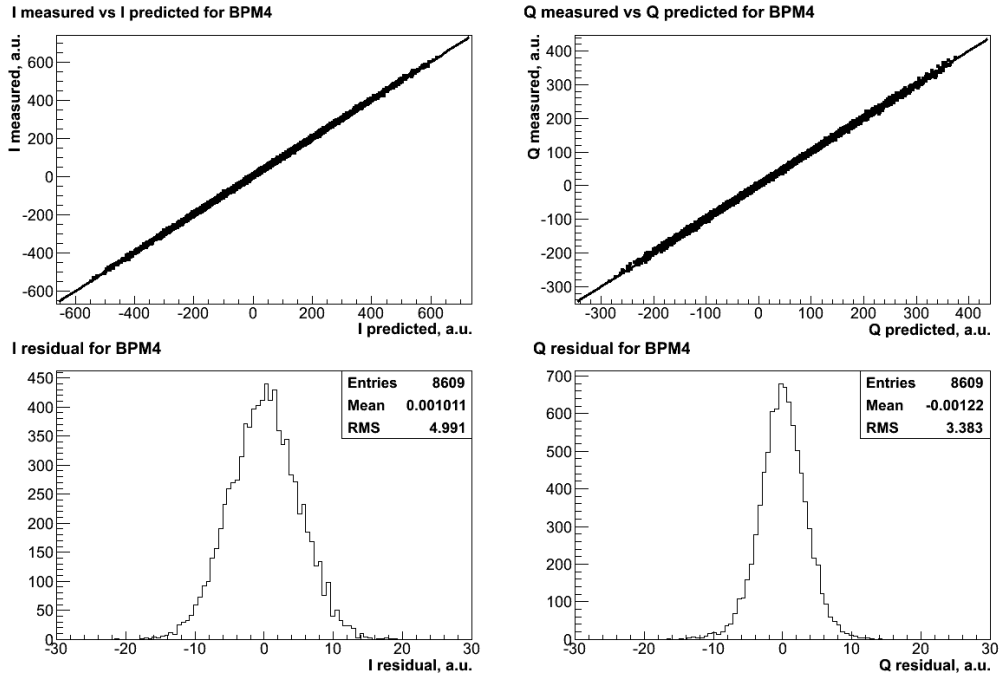


Figure 3: BPM 4 readings predicted from other BPMs in the beamline: I predicted vs I measured (top left), Q predicted vs Q measured (top right), I residual (bottom left), Q residual (bottom right).

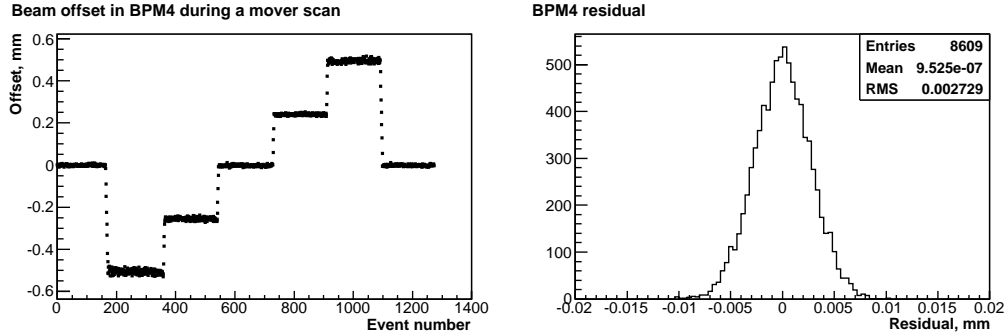


Figure 4: BPM 4 position for a horizontal mover scan (left), BPM 4 residual during a quiet period (right).

251 *3.2. Estimate of the beam energy and scale correction*

252 The I and Q readings predicted for BPM 4 by all other BPMs can be  
 253 subtracted from the measured values and, when the magnets are on, provide

254 information on how the beam trajectory changes with the energy.

255 When turning the magnets on, we also moved BPM 4 by 5 mm in order to  
 256 keep the beam centred. This movement was observed by the Zygo interferom-  
 257 eter. According to the interferometer, BPM 4 moved by 5.0034 mm between  
 258 our selected runs with magnets on and magnets off. Using the IQ rotation  
 259 and scale from the mover scan, we can predict the changes of the I and Q val-  
 260 ues of BPM 4. This results in offsets of  $I_0 = -8784$  and  $Q_0 = -4605$ , which  
 261 were added to the I and Q values from the energy scan after the predictions  
 262 had been subtracted (fig. 5, top left).

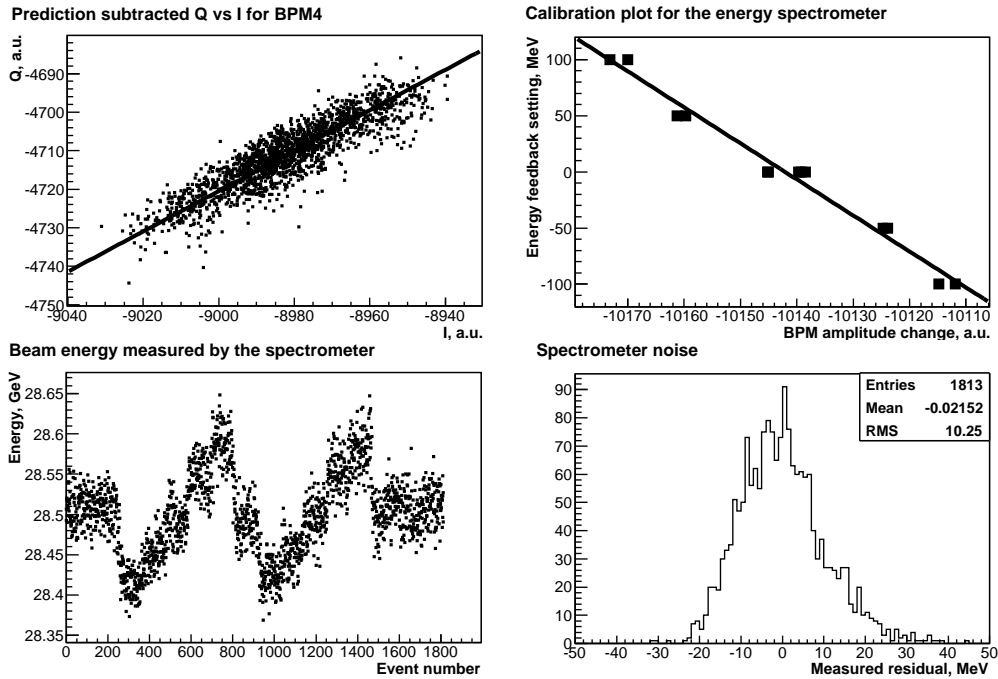


Figure 5: Beam energy measurements: prediction subtracted Q vs I for BPM 4 (offset by  $Q_0$  and  $I_0$  to take into account the 5.0034 mm move), the “energy line” fits the measured points (top left), energy calibration plot for the spectrometer (top right), beam energy measured during the scan (bottom left), spectrometer noise measured off the energy line (bottom right).

263 Although a small inclination of the beam orbit is introduced along with  
 264 the offset in the middle of the chicane due to small differences between the  
 265 magnets, the measured points still lie on a straight line in the IQ plane as  
 266 both the offset and inclination scale with the energy. Fitting the measured

267 data to a straight line going through the centre of coordinates, we obtain the  
268 IQ rotation of this “energy line”. Energy readings for each point are then  
269 calculated as a projection onto the energy line.

270 In order to get the energy scale, individual readings are averaged for each  
271 step of the energy scan and then fitted to a straight line (fig. 5, top right).  
272 The slope of this line gives the energy scale and the offset – the measured  
273 nominal energy. This procedure results in a beam energy of about 32.6 GeV,  
274 while, as mentioned above, it was kept within  $\pm 1\%$  off 28.5 GeV during the  
275 run. Although the fit may contribute up to 1.4 GeV uncertainty, introduced  
276 by the drifts during the energy scan, the difference is mainly due to the scale  
277 of the energy feedback, which was not re-calibrated for the run.

278 Introducing the values for the total beam offset  $x = 5.117$  mm, distance  
279 between the magnets  $L = 4.014$  m, and magnetic field integral  $\int Bdl =$   
280  $0.117$  T·m into eq. (1) results in a value lower than expected, 27.5 GeV.  
281 Nevertheless, this estimate confirms that the beam energy was not as high  
282 as measured using the uncorrected energy feedback scale. As measuring the  
283 absolute beam energy is out of the scope of this study, and some systematic  
284 offsets may contribute to  $E_b$ , we assume a nominal beam energy of 28.5 GeV  
285 in this article.

286 The ratio  $28.5/32.6$  gives a correction factor of 0.87, meaning that the en-  
287 ergy scan was actually performed in a range of  $\pm 87$  MeV instead of requested  
288  $\pm 100$  MeV, and the energy scale factor must be corrected accordingly.

289 The energy measured by BPM 4 during the scan is shown in fig. 5, bottom  
290 left. Peak fluctuations are less or comparable with the energy scan step size  
291 of 50 MeV, so a resolution better than 25 MeV can be expected. In the  
292 following we use the data from the energy BPMs in order to separate the  
293 energy fluctuations from noise, and include additional data acquired with the  
294 setup, such as interferometer and NMR readings, to refine the measurement  
295 and estimate the resolution of the spectrometer.

296 The last plot in fig. 5 (bottom right) shows the distribution of the offsets  
297 of the measured points from the fitted line. The RMS of the distribution is  
298 10 MeV, or 8.7 MeV ( $3.1 \cdot 10^{-4}$ ) taking into account the scale correction. This  
299 value reflects the noise performance of the BPM system since the energy- and  
300 position-induced changes act along the energy line (the incline, although not  
301 always negligible, is very small). However, it does not include the effect of  
302 the magnetic field, beam position fluctuations and associated non-linearities.  
303 Indeed, the resolution estimate of  $5.5 \cdot 10^{-4}$  obtained using position data (see  
304 section 3.1) is larger.

305 *3.3. Resolution of the energy BPMs*

306 We could only perform a relative energy measurement with BPMs 12  
307 and 24, as the field of the bending magnets in the A-line could not be turned  
308 off. However, we were still able to calibrate the energy BPMs using the energy  
309 scan data and taking into account the energy feedback scale correction.

310 Similarly to spectrometer data, we measured the RMS residual between  
311 the fitted energy line and the measured points for the energy BPMs 12 and 24.  
312 The measured noise is equivalent to 0.36 MeV for BPM 12 and 2.0 MeV for  
313 BPM 24, or  $1.3 \cdot 10^{-5}$  and  $7.0 \cdot 10^{-5}$  respectively, at the nominal beam energy  
314 of 28.5 GeV. The values are different because BPM 12 had an additional  
315 20 dB amplifier installed in its electronics chain in order to compensate for  
316 cable losses. As a consequence, this BPM's sensitivity was improved and the  
317 impact of the noise and granularity introduced by the digitisers was reduced.

318 Again, these estimates only take into account the noise in the BPMs, but  
319 not other effects such as the beam jitter and magnetic fields changes. In  
320 fig. 6 we compare the energy readings of BPMs 12 and 24 after the energy  
321 calibration. An RMS residual of 4.8 MeV ( $1.7 \cdot 10^{-4}$ ) was found, which is  
322 about twice bigger than the noise measurements combined in quadrature.  
323 This means that the resolution of the energy measurements of BPMs 12 and  
324 24 is, in fact, not limited by the BPM noise alone. Nevertheless, BPMs 12  
325 and 24 still allow energy fluctuations to be measured to better than  $1.7 \cdot 10^{-4}$ ,  
326 which is well below the expected spectrometer resolution.

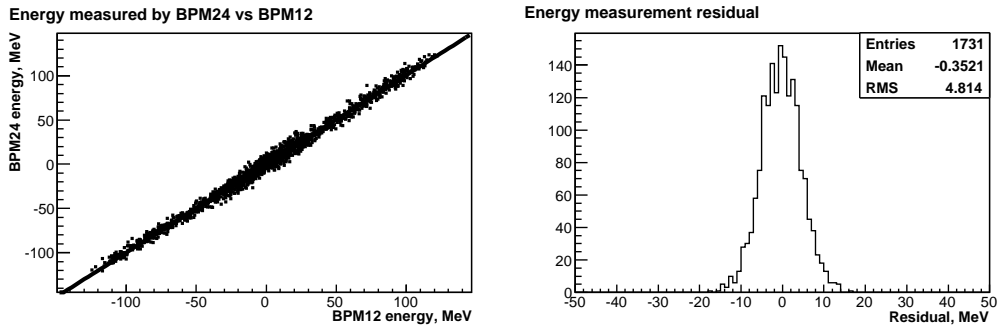


Figure 6: Comparison of BPMs 12 and 24: BPM 24 vs BPM 12 energy measurement (left), residual between BPM 12 and 24 measurements (right).

327 *3.4. Dipole magnets*

328 An essential prerequisite for the operation of the spectrometer in a Linear  
 329 Collider is that the beam position downstream of the chicane is not energy  
 330 dependent, and the upstream beam path is restored downstream. In other  
 331 words, the chicane has to be symmetric. In a 4-magnet chicane it is also  
 332 beneficial to match the magnets in each pair producing a parallel translation  
 333 of the beam (a “dogleg”), so that the inclination of the orbit with respect to  
 334 the original is kept to a minimum.

335 Magnetic field measurements were performed in March 2007. Some re-  
 336 sults are shown in fig. 7. Here, the differences between the measured and  
 337 nominal magnetic fields are plotted as a function of the nominal value for  
 338 both negative and positive polarities.

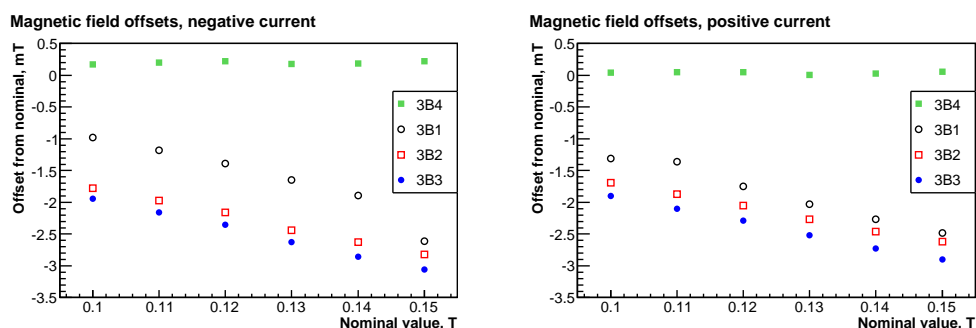


Figure 7: Offsets between the measured and nominal magnetic fields as a function of the nominal value of the four magnets in ESA: Negative current (left); Positive current (right).

339 During these measurements the field of the magnet 3B1 was monitored  
 340 with a Hall probe, whereas for the other magnets NMR probes were used. As  
 341 can be seen, 3B1, 3B2 and 3B3 follow the same trend, with a difference of a  
 342 few tenths of a mT between 3B2 and 3B3, while 3B1 differs by about 1 mT.  
 343 Offsets between these magnets can be explained by the individual history and  
 344 core composition of each (see [7] for details). 3B4 shows a different and much  
 345 more consistent behaviour, because only for this magnet a more accurate  
 346 relation between the current and the field (as given in [7]) was determined  
 347 and used for the field settings. Unfortunately, the analogous measurements  
 348 could not be preformed for the other magnets due to time constraints.

349 Due to the differences between the magnets, the trajectory of the beam  
 350 had a small inclination in the middle of the chicane and was not fully restored

351 downstream of the chicane, resulting in energy changes being converted into  
 352 position variations in BPMs 9, 10 and 11.

353 Using the data from the upstream BPMs the nominal beam position in  
 354 the downstream BPMs can be predicted. Considering, for example, BPM 9  
 355 measurements after subtraction of the upstream BPMs prediction, we can  
 356 recognise the step-like behaviour of the energy during the scan (fig. 8). Note  
 357 that, although the net integral field applied to the beam by the chicane is  
 358 very small, BPM 9 is still able to resolve the energy changes due to its high  
 359 resolution.

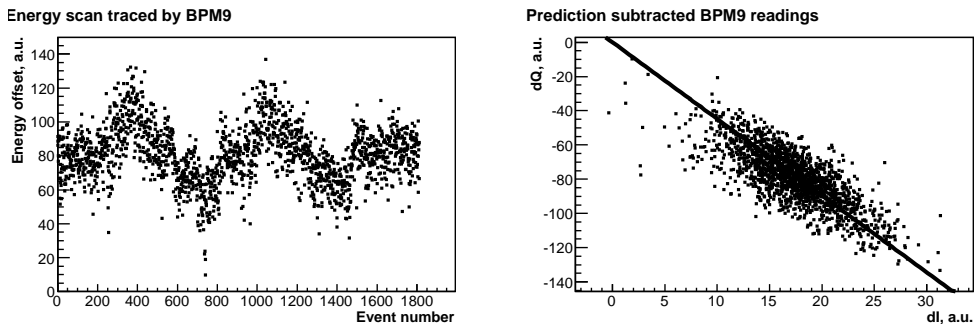


Figure 8: Energy measured by BPM 9 during the scan (left), IQ plot of the measured BPM 9 readings with the predicted readings subtracted (right). The fitted line shows the IQ rotation of the energy measurements.

### 360 3.5. Energy resolution of the spectrometer

361 The energy measured by the spectrometer can also be predicted by the  
 362 energy BPMs 12 and 24. The residual, besides the resolutions of each BPM,  
 363 depends on the fluctuations of the magnetic fields, mechanical vibrations, as  
 364 well as drifts and other systematic effects and non-linearities.

365 We first compare the relative energy measured by BPM 4 with the mea-  
 366 surements of BPM 12 (fig. 9, top). This results in a resolution of 24 MeV or  
 367  $8.4 \cdot 10^{-4}$ . As this is worse than the precision of the orbit reconstruction, we  
 368 decided to look for correlations using additional data and applying the SVD  
 369 method by starting again from BPM 12 and then adding more data in the  
 370 matrix to better reconstruct the spectrometer measurements and understand  
 371 the systematics.

372 Each time we added another parameter to the matrix, we re-calculated the  
 373 SVD coefficients from the energy scan data and then applied them to the data

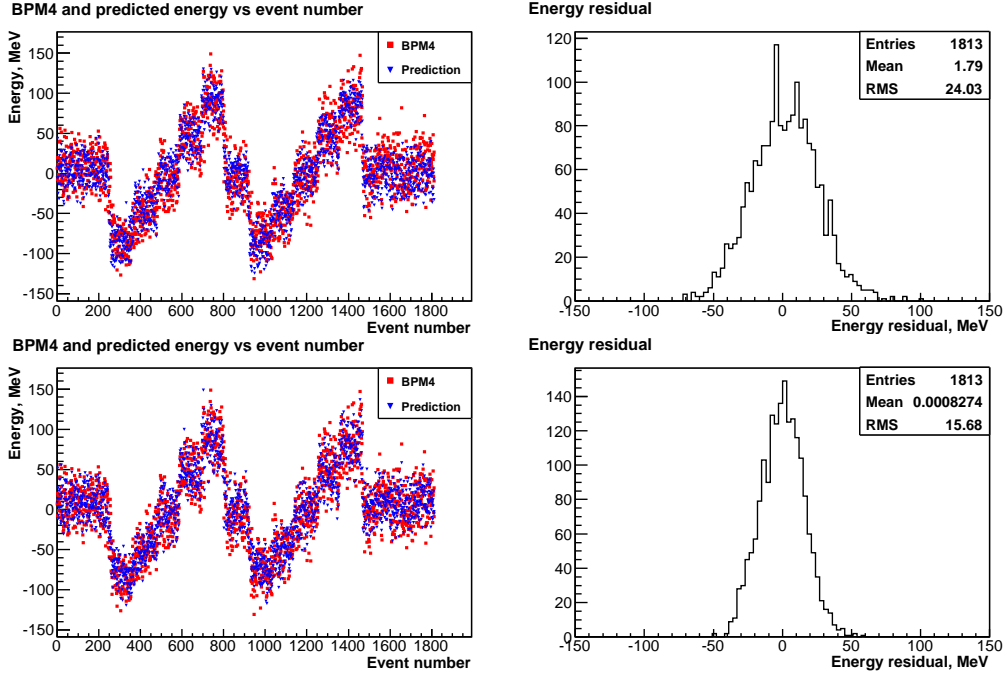


Figure 9: Energy resolution measurement: energy measured by BPM 12 and BPM 4 (top left), residual between BPM 12 and BPM 4 readings (top right), energy measurement predicted by BPMs 12, 24 and additional parameters and BPM 4 reading (bottom left), residual between the prediction and BPM 4 reading (bottom right).

374 from the quiet period. For both data sets we calculated the residual (table 1).  
 375 Note that this time when we compare BPM 4 and BPM 12 measurements  
 376 the scale is corrected by the SVD for a better match, which results in a lower  
 377 residual.

378 Where the residual is improved for both the energy scan and quiet period,  
 379 we can conclude that the uncertainty associated with the included param-  
 380 eter is reduced. We also estimate that uncertainty ( $\Delta\sigma/\sigma$ ) subtracting the  
 381 residuals ( $r$ ) in quadrature and normalising the result by the nominal energy:  
 382  $\Delta\sigma/\sigma = \sqrt{(r_{previous}^2 - r_{current}^2)}/E_b$ . These estimates are also shown in table 1.  
 383 The biggest step in residual reduction is observed when the data from BPMs  
 384 9, 10 and 11 are included in the computation. As we know, BPMs 9, 10  
 385 and 11 are sensitive to the energy, but also to the net magnetic field of the  
 386 chicane. Since our system did not provide bunch-to-bunch magnetic field  
 387 measurements, only interpolated field data could be used. Inclusion of such

388 data in the analysis did not provide a consistent improvement. It is there-  
389 fore very likely that rapid field changes are encoded in the downstream BPM  
390 data, which might be the reason for improved residuals when their data are  
391 included in the SVD matrix.

392 Some further improvement is also noted when the bunch charge  $q$ , as  
393 measured by one of the reference cavities, is taken into account, even though  
394 all the BPM data were normalised by the charge. This is best explained by  
395 the fact that BPMs 12 and 24, although very sensitive to energy changes, were  
396 not centred in their operating ranges, and were running close to saturation.

397 Ultimately, in order to achieve an energy resolution approaching  $10^{-5}$ ,  
398 one has to monitor the relative motion of the BPMs in the beamline. An  
399 interferometer, once well tuned, seems to be a reliable, fast and precision  
400 tool. Since the mechanical vibrations observed were in the order of a few  
401 hundred nanometres, the Zygo interferometer in our setup only provided a  
402 moderate improvement to the energy measurement.

403 The final result of these investigations is shown in the bottom part of  
404 fig. 9. The resolution was measured to 15.7 MeV ( $5.5 \cdot 10^{-4}$ ) for an energy  
405 scan and 14.6 MeV ( $5.1 \cdot 10^{-4}$ ) for a quiet period. These numbers are in a  
406 good agreement with the estimate for the precision of the orbit reconstruction  
407 of  $5.5 \cdot 10^{-4}$ , which means that the weighting of different systematics has been  
408 performed correctly.

### 409 *3.6. X to Y coupling*

410 Even though the spectrometer chicane operates in the horizontal plane,  
411 the energy scan is also traced in the vertical plane. Firstly, alignment errors  
412 generate a small bend in the vertical direction and, secondly, internal cross-  
413 talk between the  $x$ - and  $y$ -couplers of the BPMs create a spurious offset in  $y$   
414 due to an offset in  $x$ .

415 In order to estimate the cross-coupling between the  $x$ - and  $y$ -coordinates  
416 we again consider the energy scan data, this time to predict the vertical beam  
417 position in BPM 4 using the SVD coefficients obtained from the run with  
418 magnets off. Clearly, as seen in fig. 10 (left), the energy scan is traced in the  
419 measured  $y$ -offset. Due to different sensitivities of the  $x$ - and  $y$ -channels in  
420 BPM 4, we used mover scan data in both directions to get the position scales,  
421 which are used to normalise the raw energy. For that reason the energy is  
422 given in terms of mm in fig. 10. One should, however, keep in mind that  
423 an energy change generates both a different offset and an inclination in the  
424 mid-chicane.



Table 1: Energy residuals calculated for BPM 4 including additional parameters.  $\Delta\sigma/\sigma$  is the uncertainty calculated as two consequent residuals subtracted in quadrature and normalised by the nominal beam energy.

Data included	Residual, MeV		$\Delta\sigma/\sigma, \times 10^{-4}$	
	energy scan	quiet period	energy scan	quiet period
BPM 12	23.45	21.53	–	–
BPMs 12, 24	23.08	21.64	1.5	0.8 (up)
BPMs 12, 24 and NMR	22.67	22.62	1.5	2.3 (up)
BPMs 12, 24, NMR and fluxgate	22.67	22.62	–	–
BPMs 12, 24, charge (q), NMR and fluxgate	20.52	19.68	3.4	3.9
BPMs 12, 24, 9, 10, 11, q, NMR and fluxgate	15.86	15.26	4.6	4.4
BPMs 12, 24, 9, 10, 11, q, NMR, fluxgate and interferometer	15.68	14.60	0.8	1.6

425 The plot on the right-hand side in fig. 10 shows the correlation between  
 426 the energy measured in both planes. From the inclination of the line fitting  
 427 the data points a rotation of BPM 4 of almost  $25^\circ$  is derived, or an  $x$ - $y$   
 428 isolation of about 7.6 dB. Even without tuning, BPMs usually provide an  
 429 isolation of 20 dB, which means that the cross-talk can not be explained  
 430 solely by the cross-coupling of the signals. At the same time, the rotation is  
 431 too large to be caused entirely by the alignment errors. This indicates that  
 432 both effects take place. For the future, it is therefore important to minimise  
 433 the cross-talk in the BPMs and eliminate fake offsets by careful alignment of  
 434 the spectrometer elements.

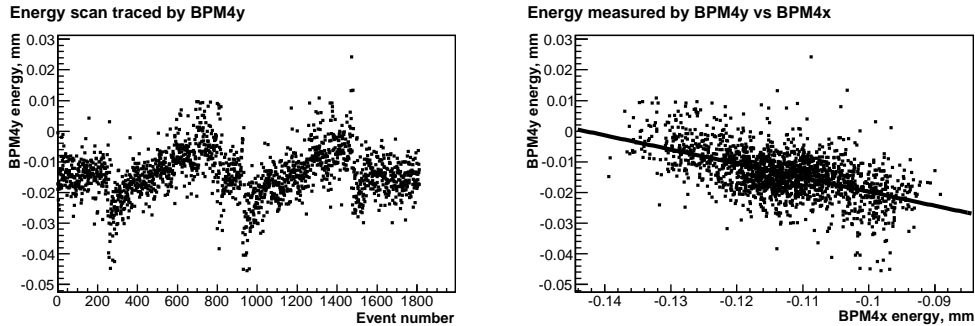


Figure 10: Effect of the chicane on the vertical beam trajectory: energy scan traced by BPM 4 in  $y$  (left), energy data measured by BPM 4 in  $y$  vs  $x$  (right). Position calibration was used to exclude the difference in sensitivities. Hence, the energy is expressed in terms of the offset (mm).

#### 435 4. Suggestions for future experiments

436 Clearly, any improvement of the BPM resolution would have a significant  
 437 positive impact on both the relative and absolute energy measurement as  
 438 it reduces the BPM uncertainties contributing to the overall measurement  
 439 error.

440 Improvement of the internal  $x$ - $y$  isolation in the BPMs would also have  
 441 a positive impact on the energy measurement as the uncertainty introduced  
 442 by the signal cross-coupled from the orthogonal direction would be smaller.

443 Higher resolution BPMs could also simplify the operation of the spectrom-  
 444 eter. For a 1 mm dispersion, a resolution of 100 nm would give a  $10^{-4}$  energy  
 445 uncertainty. Currently, a dynamic range of about 80 dB can be achieved

446 with cavity BPMs, which allows 1 mm offsets to be measured with no need  
447 to move the BPMs. Hardware improvements and better algorithms to treat  
448 the signals saturating the electronics [14] are expected to expand the dynamic  
449 range to 90 and even 100 dB. Hence, systematic effects associated with mov-  
450 ing the BPMs to track the beam when the magnets are on can be avoided  
451 without compromising the performance.

452 Without the need to move the BPMs when the chicane is in operation,  
453 the BPMs are not required to be mounted on precision movers for calibration  
454 purposes either, although simpler movers may still be mandatory for align-  
455 ment. A direct calibration of the spectrometer can be performed by changing  
456 the phase of the RF in some accelerating modules, as it was done in our ESA  
457 experiment. Another way of calibration is to change the magnetic field by a  
458 small but known amount and restore the energy scale from the orbit changes.

459 Working with I and Q values of the BPMs directly, we realised that even  
460 a 4-magnet chicane does not generate a pure beam offset in the middle of the  
461 chicane because of small differences between the magnets. At the required  
462 level of precision the inclination still needs to be taken into account. Futher-  
463 more, two magnets contribute to the uncertainty of the energy measurement  
464 in a 4-magnet chicane.

465 These arguments suggest a return to the original 3-magnet chicane de-  
466 sign as discussed in [4] and shown in fig. 11, where the central magnet, the  
467 spectrometer magnet, is instrumented with probes and the other two help  
468 to preserve the initial beam trajectory. High-precision BPMs in between the  
469 magnets provide information on the bend of the beam, while BPMs upstream  
470 of the first magnet predict the default trajectory downstream. In this case,  
471 the spectrometer magnet produces a combination of offset and angle in the  
472 BPMs downstream, but all measured data should still lie on one line in the  
473 IQ space as in our analysis, see section 3.2.

474 Instrumenting the ancillary magnets and extending the interferometer  
475 onto the up- and downstream BPMs would provide redundant energy mea-  
476 surement at a low increment in cost. While the overall resolution is not  
477 expected to become improved as the ancillary magnets operate at half of the  
478 magnetic field of the spectrometer magnet, some systematic effects can be a  
479 priori excluded due to the opposite bend. Also, BPM triplets instead of dou-  
480 blets in between the magnets would also provide redundancy of beam orbit  
481 measurements and improve both the precision and accuracy of the spectrom-  
482 eter.

483 To predict the default trajectory in a 3-magnet spectrometer, the IQ

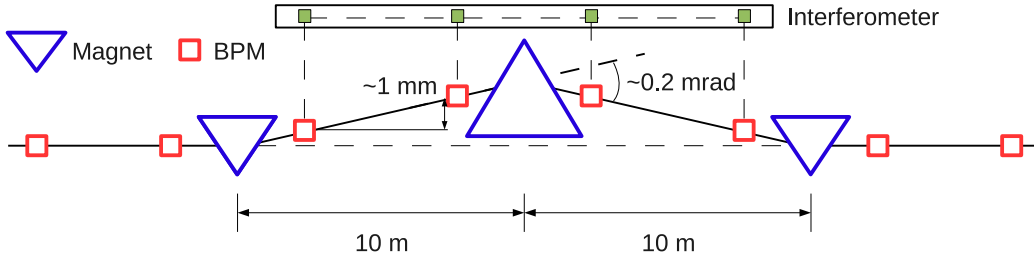


Figure 11: A 3-magnet spectrometer chicane.

484 space of the BPMs can be scanned by changing the beam deflection of the  
 485 ancillary magnets, while the spectrometer magnet is off.

486 A precision interferometer will be required to achieve the  $10^{-4}$  or better  
 487 beam energy uncertainty. This becomes critical for a reduced dispersion as  
 488 the BPM resolution must be enhanced to 100 nm, since RMS vibrations  
 489 measured at ESA were about 300 nm for stationary BPMs and approached  
 490  $1 \mu\text{m}$  for BPMs mounted on the movers. The Zygo interferometer fulfils the  
 491 requirements of the energy spectrometer, hence the vibrations should not  
 492 present a problem in future installations.

493 The resolution of the spectrometer also depends on the availability of  
 494 bunch-by-bunch magnetic field measurements. The time resolution of the  
 495 NMR probes is in the order of tens of milliseconds, which is sufficient for  
 496 bunch train averaged measurements in a linear collider, but not for bunch-  
 497 by-bunch operation. Stabilised low-noise power supplies for the magnets,  
 498 dedicated readout for each probe (no multiplexing), and combination of NMR  
 499 and Hall probes will help improving the accuracy of the bunch-by-bunch  
 500 measurements.

## 501 5. Summary

502 The model-independent analysis of the data obtained with the prototype  
 503 Linear Collider spectrometer based on a magnetic chicane achieved a res-  
 504 olution of  $5.5 \cdot 10^{-4}$  using a BPM system with a micrometre level precision  
 505 of the beam orbit measurements. An improved BPM resolution is the key  
 506 factor to enhance the energy resolution. To achieve the  $10^{-4}$  level, fast and  
 507 reliable monitoring of the magnetic field and relative motion of the BPMs in  
 508 the horizontal plane are also mandatory.

509 Novel signal processing and analysis techniques allow the BPM resolution  
510 to be pushed to the 100 nm level and below, while enhancing the dynamic  
511 range of cavity BPMs beyond the current limit of approximately 80 dB, so  
512 that large beam offsets can still be measured. This means that the dispersion  
513 in the chicane, and hence the beam emittance degradation caused by the  
514 spectrometer, can be significantly reduced. Further improvements of the  
515 BPM resolution and their dynamic range would allow operation of the chicane  
516 without BPM movers, eliminating associated systematic errors.

517 Working with uncalibrated in-phase and quadrature BPM readings, one  
518 does not have to distinguish between the beam angle and offset changes in  
519 the middle of a 4-magnet chicane. Both the angle and offset follow the en-  
520 ergy changes, and the IQ readings produce a straight line in the IQ plane.  
521 For simplicity reasons, a 3-magnet chicane becomes a preferred configura-  
522 tion. However, in this case an energy calibration of the whole system becomes  
523 necessary. Hence, any reference to a well known physics quantity, such as the  
524 Z-mass, or a complementary method to measure  $E_b$ , is important for both  
525 the scale corrections of the relative measurements and establishing the offset  
526 for absolute energy measurements.

## 527 References

- 528 [1] J. Brau, (ed. ), et al., International Linear Collider reference design  
529 report, Volume 2: Physics at the ILC, ILC Global Design Effort and  
530 World Wide Study, ILC-REPORT-2007-001 (2007).
- 531 [2] J. Brau, (ed. ), et al., International Linear Collider reference design  
532 report, Volume 3: Accelerator, ILC Global Design Effort and World  
533 Wide Study, ILC-REPORT-2007-001 (2007).
- 534 [3] R. Assmann, et al., Calibration of centre-of-mass energies at LEP2 for  
535 a precise measurement of the W boson mass, Eur. Phys. J. C39 (2005)  
536 253–292.
- 537 [4] V. N. Duginov, et al., The beam energy spectrometer at the Interna-  
538 tional Linear Collider, DESY LC Note, LC-DET-2004-031 (2004).
- 539 [5] M. Slater, et al., Cavity BPM system tests for the ILC energy spec-  
540 trometer, Nucl. Instrum. Meth. A592 (2008) 201–217.

- 541 [6] N. Morozov, Progress report on developments of the magnetic field mea-  
542 surement techniques, Beam Energy Measurement Meetings 21-23 May  
543 and 21-23 November, Yerevan, Armenia and DESY Zeuthen, Germany  
544 (2005).
- 545 [7] M. Viti, Precise and fast beam energy measurement at the International  
546 Linear Collider, Ph.D. thesis, Humboldt-Universitaet zu Berlin, DESY-  
547 THESIS-2010-007, 2010.
- 548 [8] M. Hildreth, et al., Linear Collider – BPM-based energy spectrometer,  
549 SLAC ESA Test Beam Proposals (2004, 2006).
- 550 [9] F. C. Demerest, High-resolution, high-speed, low data age uncertainty  
551 heterodyne displacement measuring interferometer electronics, Meas.  
552 Sci. Technol. 9 (1998) 1024–1030.
- 553 [10] H. J. Schreiber, et al., Magnetic measurements and simulations of a  
554 4-magnet dipole chicane for the International Linear Collider, Particle  
555 Accelerator Conference (PAC07), Albuquerque, NM, USA (2007).
- 556 [11] S. Kostromin, M. Viti, Magnetic measurements for magnets 10D37,  
557 ILC-SLACESA Note, TN-2008-1 (2008).
- 558 [12] A. Lyapin, et al., A Prototype S-Band Cavity BPM System for the ILC  
559 Energy Spectrometer, EUROTeV Report, 2008-072 (2008).
- 560 [13] W. H. Press, et al., Numerical Recipes in C, Cambridge University  
561 Press, 1992.
- 562 [14] S. Boogert, et al., Cavity beam position monitor system for ATF2,  
563 International Particle Accelerator Conference (IPAC 10), Kyoto, Japan  
564 (2010).